Published in final edited form as:
J Pathol. 2014 July ; 233(3): 217–227. doi:10.1002/path.4344.

Targeted next-generation sequencing of cancer genes dissects the molecular profiles of intraductal papillary neoplasms of the pancreas

Eliana Amato[1,*], **Marco dal Molin**[2,3,*], **Andrea Mafficini**[1,*], **Jun Yu**[2], **Giuseppe Malleo**[3], **Borislav Rusev**[1], **Matteo Fassan**[1], **Davide Antonello**[1], **Yoshihiko Sadakari**[2], **Paola Castelli**[4], **Giuseppe Zamboni**[1,4], **Anirban Maitra**[2], **Roberto Salvia**[3], **Ralph H. Hruban**[2], **Claudio Bassi**[3], **Paola Capelli**[1], **Rita T. Lawlor**[1], **Michael Goggins**[2], and **Aldo Scarpa**[1]

[1]ARC-Net Research Centre and Department of Pathology and Diagnostics, University and Hospital Trust of Verona, 37134 Verona, Italy

[2]Department of Pathology, Sol Goldman Pancreatic Research Center, Johns Hopkins Medical Institution, 21231 Baltimore, MD, USA

[3]Department of Surgery, General Surgery B, University of Verona, 37134 Verona, Italy

[4]Department of Pathology, Ospedale Sacro Cuore, 37024 Negrar, Italy

Abstract

Intraductal neoplasms are important precursors to invasive pancreatic cancer and an opportunity to detect and treat pancreatic neoplasia before an invasive carcinoma develops. The diagnostic evaluation of these lesions is challenging as diagnostic imaging and cytological sampling do not provide accurate information on lesion classification, the grade of dysplasia or the presence of invasion. Moreover, the molecular driver gene mutations of these precursor lesions have yet to be fully characterized. Fifty-two intraductal papillary neoplasms, including 48 intraductal papillary mucinous neoplasms (IPMNs) and 4 intraductal tubulopapillary neoplasms (ITPNs), were subjected to the mutation assessment in 51 cancer-associated genes, using Ion Torrent semiconductor-based next-generation sequencing. P16 and Smad4 immunohistochemistry was performed on 34 IPMNs, and 17 IPMN-associated carcinomas. At least one somatic mutation was observed in 46/48 (96%) IPMNs; 29 (60%) had multiple gene alterations. *GNAS* and/or *KRAS* mutations were found in 44/48 (92%) of IPMNs. *GNAS* was mutated in 38/48 (79%) IPMNs, *KRAS* in 24/48 (50%), and these mutations coexisted in 18/48 (37.5%) of IPMNs. *RNF43* was the

Correspondence to: Aldo Scarpa, MD, PhD, ARC-Net Research Centre, Department of Pathology & Diagnostics, University of Verona, Policlinico GB Rossi, Piazzale L.A. Scuro, 10, 37134 Verona, Italy. Tel.: +390458124043, Fax:+390458127432, aldo.scarpa@univr.it.
*shared first authorship

Potential competing interests: The authors have no competing interests to declare.

Author Contribution statement: AS, MF, RHH and AMaitra conceived the study. EA and MdM designed the study. MG, JY, and MdM designed the validation experiment. MG supervised the validation experiment. RTL coordinated patients and sample data management and supervised ethical protocols. GM, RS and CB collected materials and clinical data. BR, MF, PCapelli, GZ, AS analysed histopathological data. MF, BR, PCastelli microdissected samples. EA, MdM, JY, DA and YA carried out deep sequencing and raw data analysis. AMafficini and JY performed bioinformatic analysis. MF, PCastelli and GZ analysed immunohistochemistry. EA, AMafficini, MF and MdM drafted the manuscript. AMafficini, MG, RHH, AMaitra and RTL revised the manuscript. AS finalised the paper. All authors approved the submitted version.

third most commonly mutated gene and was always associated with *GNAS* and/or *KRAS* mutations, as were virtually all the low frequency mutations found in other genes. Mutations in *TP53* and *BRAF* genes (10% and 6%) were only observed in high-grade IPMNs. P16 was lost in 7/34 IPMNs and 9/17 IPMN-associated carcinomas; Smad4 was lost in 1/34 IPMN and 5/17 IPMN-associated carcinomas. In contrast to IPMNs, only one of four ITPN had detectable driver gene (*GNAS* and *NRAS*) mutations. Deep sequencing DNA from 7 cyst fluid aspirates identified 10 of the 13 mutations detected in their associated IPMN. Using next-generation sequencing to detect cyst fluid mutations has the potential to improve the diagnostic and prognostic stratification of pancreatic cystic neoplasms.

Keywords

IPMN; pancreatic tumours; NGS; biomarkers

Introduction

Intraductal neoplasms of the pancreas are cystic or mass-forming epithelial neoplasms that characteristically grow primarily within the ductal system [1], and include two main groups: intraductal papillary mucinous neoplasms (IPMNs) and intraductal tubulopapillary neoplasms (ITPNs).

IPMNs are precursor lesions to invasive adenocarcinoma, accounting for 5% of pancreatic neoplasms. Epithelial morphology and mucin expression patterns define four main histologic subtypes of IPMN [2]: intestinal, gastric, oncocytic and pancreaticobiliary. Recent papers support the hypothesis of distinct pathways for carcinogenesis among the different IPMN subtypes [3,4].

Cancer is a fundamentally genetic disease, and IPMNs are no exception. IPMNs commonly harbour activating mutations in *KRAS* and *GNAS*, and inactivating mutations in *RNF43*, *CDKN2A/p16*, and *TP53*, *a*nd less commonly mutations in *BRAF*, *PIK3CA*, *STK11* and *SMAD4* [5-12]. *TP53*, *CDKN2A/p16* and *SMAD4* mutations and/or loss of expression are generally found in higher-grade lesions [13-15]. IPMNs are genetically heterogeneous [16], and different patterns of genetic alterations have been reported in the different morphologic subtypes of IPMNs: Mohri *et al*. reported *KRAS* mutations as more prevalent in gastric type than in intestinal type IPMN [4]; Xiao *et al*. identified *KRAS* and *BRAF* mutations and abnormal p53 immunolabeling in the oncocytic type, but less frequently than in the pancreatobiliary IPMN [17]. Yamaguchi *et al*. analysed 15 gastric type IPMNs, pyloric gland variant, which showed frequent mutations in *GNAS* and *KRAS* (60% and 80%, respectively) [18]. ITPN is a rare variant of pancreatic intraductal neoplasms recently recognised as a distinct entity in the WHO classification [1]. A recent mutational analysis of 14 ITPN detected *PIK3CA* mutations in three cases, and one case each with *KRAS* and *BRAF* mutations, while no *GNAS* mutation was detected, suggesting a different molecular origin for ITPN [12,18].

Massive parallel sequencing, also known as next-generation sequencing (NGS) or deep sequencing can be customized to enable accurate detection of mutations in gene panels with

samples with limited DNA [19,20]. Such an approach represents a potent diagnostic complement to histopathological and immunophenotypical diagnosis [21].

In the present study we used targeted NGS to examine the mutational status of 51 cancer-related genes in 52 intraductal neoplasms of the pancreas. We also tested the diagnostic performance of NGS in cystic fluids from 10 patients with IPMN, supporting the use of NGS for classifying cyst type in clinical practice.

Materials and Methods

Cases

A retrospective series of 52 pancreatic intraductal neoplasms from 51 surgically treated patients (Table 1), including 48 IPMN and 4 ITPN with one IPMN and one ITPN coexisting in the same patient, were retrieved from the ARC-Net biobank at Verona University Hospital (www.arc-net.it). The series included 40 fresh frozen (FF) and 12 formalin-fixed paraffin-embedded (FFPE) tissues. IPMNs were classified according to WHO 2010 [1]. Dysplasia was graded as low (LG), intermediate (MG), and high grade (HG). In 10 intestinal-type IPMNs, cystic fluids were harvested from pancreatectomy specimens with a fine needle syringe, and stored at −80°C within 30 min of resection. Normal pancreatic tissues were used to determine the somatic or germline nature of mutations.

Ethics

The materials have been collected under Program 853 protocol 298CE 15/02/02 and revised Program 1885 protocol 52438 23/11/2010, approved by the Verona University Hospital ethics committee. The protocols include informed consent from the patient.

DNA extraction and quantification

DNA was obtained from tissues after enrichment for neoplastic cellularity using manual microdissection. DNA was extracted using the QiAamp DNA Mini Kit (Qiagen) from frozen tissues and the QIAamp DNA FFPE Tissue Kit from FFPE specimens (Qiagen). DNA from 250 μl of cystic fluid was purified by adding 3 ml of RLTM buffer (Qiagen) and then binding to an AllPrep DNA column (Qiagen) [10]. DNA was quantified and its quality assessed using NanoDrop (Invitrogen) and Qubit (Invitrogen) platforms [22]. The quality of DNA was further evaluated by PCR using the BIOMED 2 PCR multiplex protocol [23].

Deep Sequencing of Multiplex PCR Amplicons of 51 genes

Two multigene panels were used: the 50-gene Ion AmpliSeq Cancer Hotspot Panel v2 (Life Technologies) and an AmpliSeq Custom Panel investigating 7 genes. The first explores selected regions of the following 50 cancer-associated genes: *ABL1*, *AKT1*, *ALK*, *APC*, *ATM*, *BRAF*, *CDH1*, *CDKN2A*, *CSF1R*, *CTNNB1*, *EGFR*, *ERBB2*, *ERBB4*, *EZH2*, *FBXW7*, *FGFR1*, *FGFR2*, *FGFR3*, *FLT3*, *GNA11*, *GNAS*, *GNAQ*, *HNF1A*, *HRAS*, *IDH1*, *JAK2*, *JAK3*, *IDH2*, *KDR/VEGFR2*, *KIT*, *KRAS*, *MET*, *MLH1*, *MPL*, *NOTCH1*, *NPM1*, *NRAS*, *PDGFRA*, *PIK3CA*, *PTEN*, *PTPN11*, *RB1*, *RET*, *SMAD4*, *SMARCB1*, *SMO*, *SRC*, *STK11*, *TP53*, *VHL*. The custom panel was designed to target selected regions of 6 genes included in the previous panel (*BRAF*, *CDKN2A*, *GNAS*, *KRAS*, *SMAD4*, and *TP53*) and *RNF43* that

was not in the first panel. Details of the target regions for both panels are in Supplementary Table 1A&B.

Twenty nanograms of DNA were used for multiplex PCR amplification. Emulsion PCR was performed with the OneTouch DL or OneTouch2 systems (Life Technologies). The quality of the obtained library was evaluated by the Agilent 2100 Bioanalyser on-chip electrophoresis (Agilent Technologies). Sequencing was run on the Ion Torrent Personal Genome Machine (PGM, Life Technologies) loaded with 316 (50-gene panel) or 318 chips (custom panel). Data analysis, including alignment to the hg19 human reference genome and variant calling, was done using the Torrent Suite Software v.3.2 and v.3.6 (Life Technologies). Filtered variants were annotated using the SnpEff software v.3.1 and the IonReporter software v.1.6 (Life Technologies). Alignments were visually verified with the Integrative Genomics Viewer; IGV v.2.2, Broad Institute.

DNA Sanger Sequencing

KRAS (exons 2, 3), *GNAS* (exons 8, 9), *BRAF* (exon 15) and *TP53* (exons 5, 6, 7, 8), specific PCR fragments were analysed by Sanger sequencing. PCR products were purified using Agencourt AMPure XP magnetic beads (Beckman Coulter), labeled with Big Dye Terminator v3.1 (Applied Biosystems). Agencourt CleanSEQ magnetic beads (Beckman Coulter) were used for post-labeling purification., Sequence analysis was performed on an Applied Biosystems 3130xl Genetic Analyser.

Immunohistochemistry

IPMN tumour phenotypes were investigated according to WHO classification [1] by applying antibodies to mucin core proteins MUC-1 (clone DF3; 1:50; Abcam), MUC2 (clone Ccp58; 1:100; Novocastra Laboratories), MUC5AC (clone CLH2; 1:100; Novocastra Laboratories), and MUC6 (clone CLH5; 1:100; Novocastra Laboratories). The immunohistochemical expression of p53 (clone DO-1; prediluted; Immunotech), β-catenin (clone 15B8; 1:150; Sigma), CDKN2A/p16 (clone JC8; 1:100; Santa Cruz Biotechnology) and Smad4 (clone B-8; 1:200; Santa Cruz Biotechnology) was tested as a surrogate validation of deep sequencing results.

Statistical analysis

Fisher's exact test was used to compare mutational frequencies among IPMN grouped according to either histological subtype or tumour grade. *P* values of less than 0.05 were considered statistically significant.

Results

Clinico-pathological data

Fifty-two pancreatic intraductal neoplasms, comprising 48 IPMNs and 4 ITPNs, were retrieved from 51 patients as one patient had two separate lesions, an IPMN and an ITPN (Table 1, Figure 1). Of the 52 lesions, 40 (77%) were in the pancreatic head and/or the uncinate process, 9 (17%) in the pancreatic body/tail, and 3 (6%) diffusely involved the gland. Macroscopically, 31 (60%) neoplasms were main-duct type, 3 (6%) branch-duct type,

and 18 (34%) combined-type. The 48 IPMNs were classified, according to WHO classification [1], into the following subtypes: 36 intestinal, 6 gastric, 3 pancreaticobiliary and 3 oncocytic type. Invasive carcinoma was associated with the IPMN in 29 of the 51 (57%) patients: 18 of the invasive cancers were colloid carcinomas, and 11 were conventional tubular adenocarcinomas.

Tissues and cystic fluid subjected to sequencing

Non-invasive lesions from the 48 IPMN were low-grade (LG) in 3 cases, intermediate-grade (IG) in 17 cases and high-grade (HG) in 28 cases. For three IPMNs (128fp, 129fp and 138fp) sufficient material was obtained from non-invasive and invasive neoplastic areas (Table 2, Supplementary Table 2, Figure 2). One IPMN coexisted with an ITPN in the same patient (case 130fp); the two lesions were microdissected and analysed separately (Supplementary Table 2, Figure 3). All 4 ITPNs showed HG dysplasia. In 10 intestinal-type IPMNs cystic fluid was available and in 7 of these (70%) an adequate library for sequencing was obtained.

Prevalence of driver gene mutations among the 50 genes of the AmpliSeq panel

An adequate library was obtained from all samples for subsequent sequencing. Mean 100× coverage of 98.9% with a mean read length of 110 bp was obtained in the 40 FF samples and mean 100× coverage of 98.5% with a mean read length of 105 bp was obtained in the 12 FFPE samples.

GNAS and *KRAS* mutations were the most prevalent alterations, found in 39/52 (75%) and 24/52 (46%) lesions, respectively. *GNAS* and/or *KRAS* mutations were identified in 45/52 (87%) cases; concomitant *GNAS* and *KRAS* mutations were found in 18/52 (35%) cases. Most *GNAS* mutations were in codon 201 (R201C and R201H); one Q227L mutation, not previously described in IPMN was also detected; *KRAS* mutations were in codon 12 in all but five cases, which were one in codon 14 (V14I) (Figure 4), one in codon 22 (Q22K), and three in codon 61 (one Q61R, two Q61H) (Supplementary Table 2).

The prevalence of mutations in the other genes sequenced was lower. Five (10%) of the 52 lesions harboured a *TP53* mutation, and three (6%) a *BRAF* mutation; mutations in *CTNNB1*, *IDH1*, *STK11*, and *PTEN* were each found in two tumours (2/52, 4%); *ATM*, *CDH1*, *CDKN2A*, *FGFR3*, *NRAS*, *SMAD4*, and *SRC* gene mutations were each found in only one of the 52 cases (1/52, 2%). All these genes were mutated in association with *GNAS* and/or *KRAS* mutations, with the exception of two IPMNs, one that only had a *FGFR3* mutation and another that only had a *TP53* mutation (Supplementary Table 2). The five *TP53* mutated lesions included a frame-shift deletion (N247_R249del), a stop mutation at codon 306 (R306X), and the non-synonymous variants R175H, I195N, and V272L in exons 5 and 6. *BRAF* was mutated at the hotspot codons 599-601 (T599delinsIP, VK600E, and K601E) in exon 15. Most samples contained germline non-pathogenic variants in one or more of the following genes: *PIK3CA*, *KIT*, *TP53*, *ATM*, *MET*, *KDR*, *FGFR3*, and *APC* (data not shown).

Validation of mutations in six genes and screen for *RNF43* mutations using an AmpliSeq custom panel

Forty-two of the 52 DNA samples (33 FF, 9 FFPE) were re-analysed using a custom gene panel to confirm the mutations in six genes (*BRAF*, *CDKN2A*, *GNAS*, *KRAS*, *SMAD4*, *TP53*) and to evaluate the role of *RNF43*, *a* gene that was not included in the first gene panel. An adequate library for subsequent sequencing was obtained for all samples. Mean 100× coverage of 100% with a mean read length of 175 bp was achieved in the 33 FF samples and mean 100× coverage of 99.24% with a mean read length of 150 bp was achieved in the 9 FFPE samples.

All the mutations identified in the first analysis were confirmed, with negligible variations of allelic frequencies (Supplementary Table 3); an additional mutation in *CDKN2A* (A148T) was detected due to the longer region of gene covered by the custom panel. Mutations in *RNF43* gene were detected in six of the 42 samples (14%), and included: one deletion (M18Pfs*31) in exon 2, two insertions (R117Qfs*8 and E258*) in exons 3 and 7, respectively, and two missense variants (N179K) in exon 5 and exon 9 (S321I), and one nonsense (R371*) in exon 9.

Validation of mutations in five genes using Sanger sequencing and immunohistochemistry

Mutations in *KRAS* (exons 2, 3), *GNAS* (exons 8, 9), *BRAF* (exon 15), and *TP53* (exons 5, 6, 7, 8) detected by deep sequencing were all confirmed by Sanger sequencing. We used p53 and β-catenin nuclear immunolabeling as a surrogate validation for *TP53* and *CTNNB1* mutational status. For *TP53*, cases 114, 939 and 138fp showed abnormal p53 nuclear accumulation of the mutated protein; cases 106 and 108, respectively harbouring the N247_R249del frame-shift deletion and the homozygous R306X mutation, had no immunolabeling (Figure 5). Two *CTNNB1* mutated cases had nuclear immunopositivity for β-catenin.

Evaluation of *CDKN2A/P16* and *SMAD4* dysregulation using immunohistochemistry

Immunohistochemistry was used as a surrogate test to assess the involvement of *CDKN2A/P16* and *SMAD4* genes [7,24,25]. In fact, protein expression may more accurately reflect gene status as both genes are mainly inactivated by homozygous deletion, and *CDKN2A/P16* also by promoter methylation.

Material was available for 36 cases: 34 IPMN (23 intestinal-type, 5 gastric-type, 3 pancreaticobiliary, and 3 oncocytic-type) and 2 ITPN. In 17 IPMN the non-invasive lesion coexisted with invasive carcinoma, for a total of 53 lesions analysed (i.e., 34 IPMN, 2 ITPN, 17 invasive carcinoma).

In normal pancreatic parenchyma, p16 was expressed in Langerhans' islets, and in random acinar and duct cells (Figure 6). P16 loss was observed in 19/53 (36%) lesions distributed as follow: 0/1 (0%) LG, 3/13 (23%) IG, 7/22 (31%) HG, and 9/17 (53%) invasive carcinomas. Most p16-loss cases (9/10) were intestinal-type IPMNs. Only 1 of the 2 *CDKN2A/P16* mutated IPMNs was available for immunophenotyping, and it lacked p16 expression.

Normal pancreatic parenchyma showed a strong nuclear and cytoplasmic Smad4 expression in all cell types including Langerhans' islets, acinar cells, stromal cells, and duct cells (Figure 6). Only 1 intestinal-type IPMN showed loss of Smad4 expression. Four IPMN-associated invasive carcinomas were Smad4 negative, with the coexisting Smad4-positive non-invasive component. Case 137fp, harbouring a F253C *SMAD4* mutation, expressed Smad4. Thus, 5/17 (29%) invasive carcinomas had Smad4 alterations.

The 2 ITPNs showed strong immunoreactions for both p16 and Smad4.

Mutation prevalence according to histological subtype

Among IPMNs, at least one somatic mutation was observed in 46/48 (96%) cases, while 29 neoplasms (60%) had multiple gene alterations (Table 3, Supplementary Table 2). *GNAS* and/or *KRAS* mutations were found in 44/48 (92%) IPMNs: *GNAS* was mutated in 38/48 (79%) cases, *KRAS* in 24/48 (50%), and these mutations coexisted in 18/48 (37.5%) cases.

All 6 gastric type IPMNs harboured a *GNAS* mutation and five of these cases also had a *KRAS* mutation (Table 3). Among intestinal type IPMNs, most harboured *GNAS* (30/36, 83%) and/or *KRAS* (14/36, 39%) mutations. The prevalence of *GNAS* mutation among gastric and intestinal IPMN subtypes was similar (P=0.568). Conversely, *KRAS* alterations were less frequent in intestinal than in gastric IPMNs, although not reaching statistical significance (P=0.075). *TP53* and *BRAF* alterations were each observed in 3 of the 36 (8%) intestinal-type IPMNs and in none of the gastric IPMNs. Among the less represented IPMN subtypes (pancreaticobiliary, n=3, oncocytic, n=3), *GNAS* and *KRAS* variants were present in the pancreaticobiliary and oncocytic IPMNs (1 of 3 *GNAS*, and 2 of 3 *KRAS*). Notably, *TP53* was mutated only in the pancreaticobiliary-type IPMNs (2 of 3). *RNF43* mutations were detected in 4 (12%) of 32 intestinal-type and one of two pancreaticobiliary-type IPMNs, and were always associated with *GNAS* and/or *KRAS* mutations. None of the gastric, oncocytic or ITPN had *RNF43* mutations.

The only mutations detected in the four ITPNs, were detected in case 130fp, where the coexisting IPMN and ITPN lesions shared the same *GNAS* R201H mutation; this ITPN also had an additional *NRAS* Q61L mutation (Supplementary Table 2, Figure 3).

Mutation prevalence according to tumour grade

Low- or intermediate-grade dysplastic samples were characterized by recurrent mutations in *GNAS* (90%) and *KRAS* (65%); while the prevalence of these mutations was significantly lower in high grade/invasive carcinoma samples (66% of the high-grade lesions harboured a *GNAS* and 34% a *KRAS* mutation, P=0.0001 and P=0.046, respectively) (Table 3). We had significantly more intestinal-type IPMNs than in the series by Wu et al. [10], and this was likely a factor in the lower prevalence of mutant *KRAS* in the IPMNs with high-grade dysplasia (Supplementary Table 2). Notably, *TP53* and *BRAF* mutations were found in high-grade lesions (15% and 9%, respectively), but not in any of the low or intermediate-grade lesions.

Mutations in matched non-invasive and invasive tumours

Three cases (128fp, 129fp and 138fp) with matched non-invasive and invasive components had similar mutational profiles (Table 2, Figure 2). Seven mutations observed in the *GNAS*, *KRAS*, *BRAF*, *KRAS* and *STK11* genes were shared between the pre-invasive and invasive lesions; three point mutations in *CDKN2A*, *SMAD4*, and *PTEN* were observed in only one of the matched lesions.

NGS can identify IPMN specific mutations in cystic fluid

DNAs from cystic fluids were available for 10 intestinal-type IPMNs, and were deep sequenced with the 50-gene AmpliSeq Cancer Panel. An adequate library was obtained in 7 cyst fluids and sequencing detected 10 of the 13 mutations present in the matched IPMN, including six of seven *GNAS* mutations, three of three *KRAS* mutations, and one of two *TP53* mutations.

Discussion

Intraductal papillary mucinous neoplasms are important precursors to invasive pancreatic cancer and represent an opportunity for detection and treatment of pancreatic neoplasia before an invasive carcinoma develops [2,26-28]. While the phenotypic classification of IPMNs is well established, the molecular drivers of this precursor lesion have yet to be fully characterized [4,12,17,29]. In this study, we explored the mutational status of 51 cancer related genes in 52 intraductal lesions, including 48 IPMN and 4 ITPN, and tested the diagnostic performance of the test on 10 cystic fluid samples.

The 48 IPMNs harboured frequent somatic mutations in *GNAS* and *KRAS*, and at least one of the two genes was mutated in 44/48 (92%) of the IPMNs. *GNAS* mutations were identified in 79% of tumours and most of them involved codon 201. *KRAS* was mutated in 50% of IPMNs, and mutations were located in codons 12, 14, 22, and 61. Our literature review finds that *KRAS* codon 14 mutations have never been reported for colorectal or pancreatic cancer. Although *KRAS* codon 14 mutations are rare, they are considered as driver in nature [30,31]. The high prevalence of *GNAS* and *KRAS* mutations found in our series is similar to that of previous studies, and suggests that these genes may be ideal targets for early detection efforts [11,32].

RNF43 was the gene with the third most frequent intragenic mutations detected by our sequencing analysis. These *RNF43* mutations were always associated with *GNAS* and/or *KRAS* mutations. Five of the six mutations detected are newly described, as only one had been previously reported for IPMN [11,32]. Our series adds to the limited literature regarding the prevalence and distribution of *RNF43* in this class of tumours, as only 8 IPMNs have been evaluated for *RNF43* mutations in the literature [10].

For other genes, mutations were detected in a small percentage (<5%) of samples in *CDKN2A*, *CTNNB1*, *IDH1*, *STK11*, *PTEN* (each one in two of the 52 tumours) and *ATM*, *CDH1*, *FGFR3*, *NRAS*, *SMAD4*, *SRC* (each one in one of the 52 neoplasms). These genes were mutated in association with *GNAS* and/or *KRAS* mutations, with the exception of two IPMNs, one IPMN that only had a *FGFR3* mutation and another that only had a *TP53*

mutation. Prior studies have reported STK11 mutations in a similar percentage of IPMNs (9%) [8]. Prior studies have found *ATM and CDH1* somatic mutations in a small percentage of pancreatic ductal adenocarcinomas but these mutations have not been yet reported in IPMNs [33,34]. Somatic mutations in *IDH1*, *PTEN* and *FGFR3*, *NRAS*, *SRC* have not been reported in IPMNs or in pancreatic ductal adenocarcinomas [33,34]. *CTNNB1* mutations are characteristic of pancreatic solid and pseudopapillary tumours, but nuclear expression of β-catenin has been described in some IPMNs [17]. The mutations we found in *IDH1*, *NRAS* and *CTNNB1* arose in known hotspots for these genes. Although *PTEN* mutations have not been previously reported in IPMNs or ITPNs [12], loss of PTEN expression in IPMNs has been reported [35], and mutations in *PIK3CA*, another gene in this pathway also occur in a small percentage of cases [5,16,35]. The pathogenetic role of *CDKN2A/P16* and *SMAD4* was further investigated by immunohistochemical analysis. Our results demonstrated that 36% of IPMNs show loss of p16 and 24% of IPMN-related invasive carcinomas loss of Smad4, which is in accordance to previous studies [4,7].

The different histological subtypes of IPMNs showed a partial overlap in the mutational spectrum, as well as some differences. *GNAS* gene mutations were common in all types, consistent with previous reports [10,11,32,36]. *KRAS* mutations were more common in gastric-type compared to intestinal-type IPMNs (83% *vs*. 39%, *P*=0.07), as has been reported by Mohri *et al*. (82% *vs* .27%) [4]. Other authors have reported that oncocytic-type IPMNs are less likely to have *KRAS* gene mutations than pancreaticobiliary type-IPMNs [17], while in our study all three pancreaticobiliary and two of three oncocytic cases harboured *KRAS* mutations.

Three of four ITPNs had no mutations in the 50-gene panel. The ITPN that coexisted with an IPMN had mutations in both *GNAS* and *NRAS*. The mutation observed in *GNAS* is of note, because Yamaguchi and colleagues have recently reported that this gene was not mutated in a series of 14 ITPNs [18]. Previous reports found activating *PIK3CA* mutations in 3 of 14 (21%) of ITPNs [12,18]. Two different groups identified *PIK3CA* mutations in 11% (4/36) and 9% (2/21) of IPMNs, respectively [5,16]; noteworthy, the missense hot-spot mutation H1047R in exon 20 was found in 4 of 6 invasive cancers. In our series, *PIK3CA* mutations were absent in both ITPN and IPMN; given the good quality of sequences we obtained, this discrepancy is possibly due to the small number of cases analysed by each of the three studies. Although we only analysed four ITPN cases, the absence of *KRAS* and *BRAF* mutations in ITPN supports the hypothesis of a distinct molecular profile and possibly an independent origin for ITPN lesions. *TP53* and *BRAF* mutations were only found in high-grade lesions (15% and 9%, respectively), suggesting that these mutations could be a potential diagnostic marker for high-grade dysplasia.

Recent guidelines emphasize conservative management of patients with IPMNs unless there are stigmata of cancer [37], particularly for elderly patients who often have comorbid conditions that increase surgical risk. Because pancreatic imaging does not provide sufficient information about the characteristics of pancreatic cysts, fine needle is used for further evaluation, but current tests do not provide sufficient diagnostic information. Therefore, the identification of novel diagnostic approaches based on genetic analyses of cyst fluid aspirated at the time of endoscopic ultrasound is particularly appealing. In the

present study, we demonstrate that targeted next-generation sequencing is feasible with cystic fluid samples, and can provide information about the genetic profile of these lesions. Notably cyst fluid analysis identified only 10 of the 13 somatic mutations found in the corresponding IPMNs. We suspect that this was because of a low concentration of mutations in the cyst fluid, below the limit of detection of our assay and this could be related to how the cyst fluids were sampled. Further study is needed to evaluate the concentration of mutations in IPMN cyst fluids. There are other approaches that can be employed to increase the limit of detection of next-generation sequencing such as BEAMing or Safe-Seqs analysis [11,38].

The prevalence of *KRAS* mutations in our series (50%) of IPMNs is lower than that observed by Wu and colleagues, who reported 79% prevalence of *KRAS* mutations in IPMNs [11]. This difference is reflected in differences in the prevalence of the histological subtypes of IPMNs in the two series: Wu et al. studied 48 IPMNs, the majority of which were gastric-type (27 cases) and included 10 intestinal-type, 5 pancreaticobiliary-type, and 6 undetermined. Our series included 6 gastric-type and 36 intestinal-type IPMNs (see Table 3). For gastric-type IPMNs, *KRAS* mutations were found in 25/27 (93%) cases of Wu et al. and in 5/6 (83%) of our series; for intestinal-type IPMNs, they found mutations in 4/10 (40%) of cases whereas we found mutations in 14/36 (39%) of cases.

In conclusion, gastric and intestinal IPMNs commonly harbour *GNAS* and *KRAS* gene mutations that likely precede mutations in other genes that are less common in IPMNs and when found are generally more common in higher-grade lesions. Moreover, our data also confirm the suggestion that ITPN appears to be a pancreatic intraductal disease different from IPMN [12,18]. *TP53* gene mutations have been only found in higher-grade lesions, suggesting that these mutations could be a specific marker for high-grade dysplasia or invasive cancer. Next-generation sequencing of cystic fluid samples can identify the majority of mutations arising in IPMNs potentially improving the diagnostic and prognostic stratification of IPMNs.

Supplementary Material

Refer to Web version on PubMed Central for supplementary material.

Acknowledgments

We thank Dr. Samantha Bersani for her valuable help in performing immunohistochemistry. The study was supported by Italian Cancer Genome Project (FIRB RBAP10AHJB), Associazione Italiana Ricerca Cancro (AIRC grants n. 12182 and 6421), Fondazione Italiana Malattie Pancreas – Ministero Salute (CUP_J33G13000210001), National Institutes of Health CA62924, Susan Wojcicki and Dennis Troper, and the Michael Rolfe Foundation. The funding agencies had no role in the collection, analysis and interpretation of data and in the writing of the manuscript.

References

1. Adsay, NV.; Fukushima, N.; Furukawa, T., et al. Intraductal neoplasms of the pancreas. In: Bosman, FT.; Carneiro, F.; Hruban, RH., et al., editors. WHO classification of tumours of the digestive system. 4th. IARC; Lyon: 2010.

2. Luttges J, Zamboni G, Longnecker D, et al. The immunohistochemical mucin expression pattern distinguishes different types of intraductal papillary mucinous neoplasms of the pancreas and determines their relationship to mucinous noncystic carcinoma and ductal adenocarcinoma. Am J Surg Pathol. 2001; 25:942–948. [PubMed: 11420467]
3. Chadwick B, Willmore-Payne C, Tripp S, et al. Histologic, immunohistochemical, and molecular classification of 52 IPMNs of the pancreas. Appl Immunohistochem Mol Morphol. 2009; 17:31–39. [PubMed: 18813127]
4. Mohri D, Asaoka Y, Ijichi H, et al. Different subtypes of intraductal papillary mucinous neoplasm in the pancreas have distinct pathways to pancreatic cancer progression. J Gastroenterol. 2012; 47:203–213. [PubMed: 22041919]
5. Schonleben F, Qiu W, Ciau NT, et al. PIK3CA mutations in intraductal papillary mucinous neoplasm/carcinoma of the pancreas. Clin Cancer Res. 2006; 12:3851–3855. [PubMed: 16778113]
6. Abe K, Suda K, Arakawa A, et al. Different patterns of p16INK4A and p53 protein expressions in intraductal papillary-mucinous neoplasms and pancreatic intraepithelial neoplasia. Pancreas. 2007; 34:85–91. [PubMed: 17198188]
7. Biankin AV, Biankin SA, Kench JG, et al. Aberrant p16(INK4A) and DPC4/Smad4 expression in intraductal papillary mucinous tumours of the pancreas is associated with invasive ductal adenocarcinoma. Gut. 2002; 50:861–868. [PubMed: 12010891]
8. Sato N, Rosty C, Jansen M, et al. STK11/LKB1 Peutz-Jeghers gene inactivation in intraductal papillary-mucinous neoplasms of the pancreas. Am J Pathol. 2001; 159:2017–2022. [PubMed: 11733352]
9. Schonleben F, Qiu W, Allendorf JD, et al. Molecular analysis of PIK3CA, BRAF, and RAS oncogenes in periampullary and ampullary adenomas and carcinomas. J Gastrointest Surg. 2009; 13:1510–1516. [PubMed: 19440799]
10. Wu J, Jiao Y, Dal Molin M, et al. Whole-exome sequencing of neoplastic cysts of the pancreas reveals recurrent mutations in components of ubiquitin-dependent pathways. Proc Natl Acad Sci U S A. 2011; 108:21188–21193. [PubMed: 22158988]
11. Wu J, Matthaei H, Maitra A, et al. Recurrent GNAS mutations define an unexpected pathway for pancreatic cyst development. Sci Transl Med. 2011; 3:92ra66.
12. Yamaguchi H, Kuboki Y, Hatori T, et al. Somatic mutations in PIK3CA and activation of AKT in intraductal tubulopapillary neoplasms of the pancreas. Am J Surg Pathol. 2011; 35:1812–1817. [PubMed: 21945955]
13. Iacobuzio-Donahue CA, Klimstra DS, Adsay NV, et al. Dpc-4 protein is expressed in virtually all human intraductal papillary mucinous neoplasms of the pancreas: comparison with conventional ductal adenocarcinomas. Am J Pathol. 2000; 157:755–761. [PubMed: 10980115]
14. Kanda M, Sadakari Y, Borges M, et al. Mutant TP53 in duodenal samples of pancreatic juice from patients with pancreatic cancer or high-grade dysplasia. Clin Gastroenterol Hepatol. 2013; 11:719–730. e715. [PubMed: 23200980]
15. Sato N, Ueki T, Fukushima N, et al. Aberrant methylation of CpG islands in intraductal papillary mucinous neoplasms of the pancreas. Gastroenterology. 2002; 123:365–372. [PubMed: 12105864]
16. Lubezky N, Ben-Haim M, Marmor S, et al. High-throughput mutation profiling in intraductal papillary mucinous neoplasm (IPMN). J Gastrointest Surg. 2011; 15:503–511. [PubMed: 21225475]
17. Xiao HD, Yamaguchi H, Dias-Santagata D, et al. Molecular characteristics and biological behaviours of the oncocytic and pancreatobiliary subtypes of intraductal papillary mucinous neoplasms. J Pathol. 2011; 224:508–516. [PubMed: 21547907]
18. Yamaguchi H, Kuboki Y, Hatori T, et al. The discrete nature and distinguishing molecular features of pancreatic intraductal tubulopapillary neoplasms and intraductal papillary mucinous neoplasms of the gastric type, pyloric gland variant. J Pathol. 2013; 231:335–341. [PubMed: 23893889]
19. Scarpa A, Sikora K, Fassan M, et al. Molecular typing of lung adenocarcinoma on cytological samples using a multigene next generation sequencing panel. PLoS One. 2013; 8:e80478. [PubMed: 24236184]

20. Beadling C, Neff TL, Heinrich MC, et al. Combining highly multiplexed PCR with semiconductor-based sequencing for rapid cancer genotyping. J Mol Diagn. 2013; 15:171–176. [PubMed: 23274167]
21. Luchini C, Capelli P, Fassan M, et al. Next-generation histopathological diagnosis: a lesson from a hepatic carcinosarcoma. J Clin Oncol. 2014 in press.
22. Simbolo M, Gottardi M, Corbo V, et al. DNA qualification workflow for next generation sequencing of histopathological samples. PLoS One. 2013; 8:e62692. [PubMed: 23762227]
23. Zamo A, Bertolaso A, van Raaij AW, et al. Application of microfluidic technology to the BIOMED-2 protocol for detection of B-cell clonality. J Mol Diagn. 2012; 14:30–37. [PubMed: 22026958]
24. Wilentz RE, Su GH, Dai JL, et al. Immunohistochemical labeling for dpc4 mirrors genetic status in pancreatic adenocarcinomas : a new marker of DPC4 inactivation. Am J Pathol. 2000; 156:37–43. [PubMed: 10623651]
25. Wilentz RE, Geradts J, Ma ynard R, et al. Inactivation of the p16 (INK4A) tumor-suppressor gene in pancreatic duct lesions: loss of intranuclear expression. Cancer Res. 1998; 58:4740–4744. [PubMed: 9788631]
26. Furukawa T, Kloppel G, Volkan Adsay N, et al. Classification of types of intraductal papillary-mucinous neoplasm of the pancreas: a consensus study. Virchows Arch. 2005; 447:794–799. [PubMed: 16088402]
27. Nakamura A, Horinouchi M, Goto M, et al. New classification of pancreatic intraductal papillary-mucinous tumour by mucin expression: its relationship with potential for malignancy. J Pathol. 2002; 197:201–210. [PubMed: 12015744]
28. Yonezawa S, Taira M, Osako M, et al. MUC-1 mucin expression in invasive areas of intraductal papillary mucinous tumors of the pancreas. Pathol Int. 1998; 48:319–322. [PubMed: 9648163]
29. Fassan M, Simbolo M, Bria E, et al. High-throughput mutation profiling identifies novel molecular dysregulation in high-grade intraepithelial neoplasia and early gastric cancers. Gastric Cancer. 2013
30. Schubbert S, Zenker M, Rowe SL, et al. Germline KRAS mutations cause Noonan syndrome. Nat Genet. 2006; 38:331–336. [PubMed: 16474405]
31. Tyner JW, Erickson H, Deininger MW, et al. High-throughput sequencing screen reveals novel, transforming RAS mutations in myeloid leukemia patients. Blood. 2009; 113:1749–1755. [PubMed: 19075190]
32. Furukawa T, Kuboki Y, Tanji E, et al. Whole-exome sequencing uncovers frequent GNAS mutations in intraductal papillary mucinous neoplasms of the pancreas. Sci Rep. 2011; 1:161. [PubMed: 22355676]
33. Biankin AV, Waddell N, Kassahn KS, et al. Pancreatic cancer genomes reveal aberrations in axon guidance pathway genes. Nature. 2012; 491:399–405. [PubMed: 23103869]
34. Jones S, Zhang X, Parsons DW, et al. Core signaling pathways in human pancreatic cancers revealed by global genomic analyses. Science. 2008; 321:1801–1806. [PubMed: 18772397]
35. Garcia-Carracedo D, Turk A, Fine S, et al. Loss of PTEN expression predicts poor prognosis in patients with intraductal papillary mucinous neoplasms of the pancreas. Clin Cancer Res. 2013; 19:6830–6841. [PubMed: 24132918]
36. Dal Molin M, Matthaei H, Wu J, et al. Clinicopathological Correlates of Activating GNAS Mutations in Intraductal Papillary Mucinous Neoplasm (IPMN) of the Pancreas. Ann Surg Oncol. 2013; 20:3802–3808. [PubMed: 23846778]
37. Tanaka M, Fernandez-del Castillo C, Adsay V, et al. International consensus guidelines 2012 for the management of IPMN and MCN of the pancreas. Pancreatology. 2012; 12:183–197. [PubMed: 22687371]
38. Kinde I, Wu J, Papadopoulos N, et al. Detection and quantification of rare mutations with massively parallel sequencing. Proc Natl Acad Sci U S A. 2011; 108:9530–9535. [PubMed: 21586637]

Abbreviations

IPMN	intraductal papillary mucinous neoplasms
ITPN	intraductal tubulopapillary neoplasms
WHO	World Health Organisation

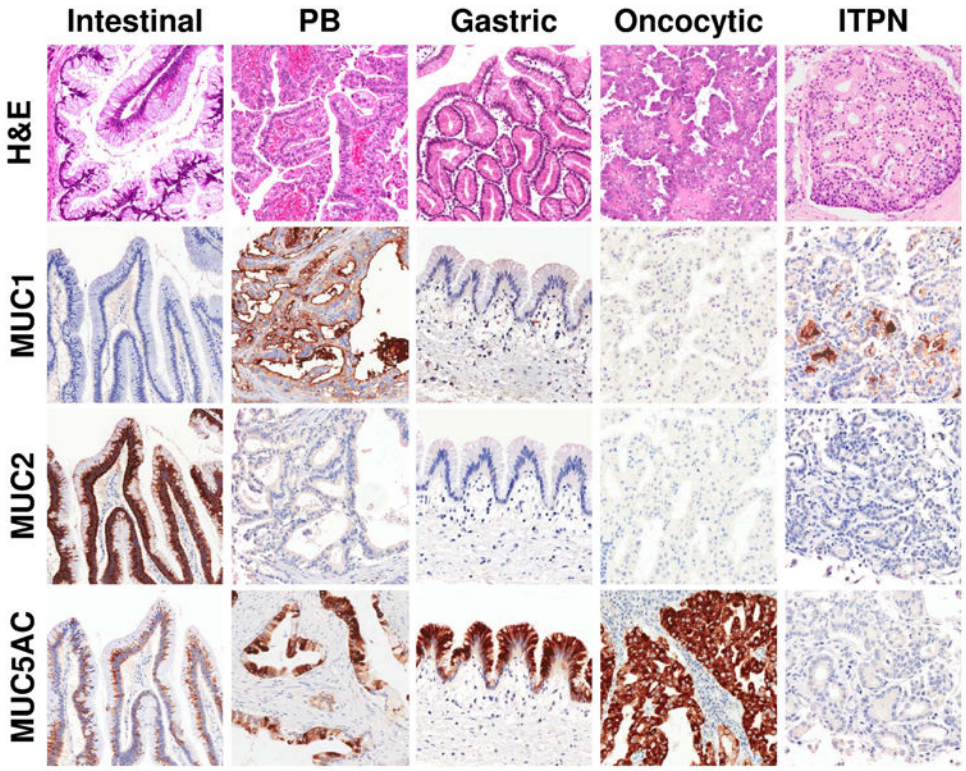

Figure 1.

Representative haematoxylin-eosin images and differential mucins immunolabeling of pancreatic intraductal neoplasms (original magnifications 20×). PB, Pancreaticobiliary; ITPN, intraductal tubulopapillary neoplasm.

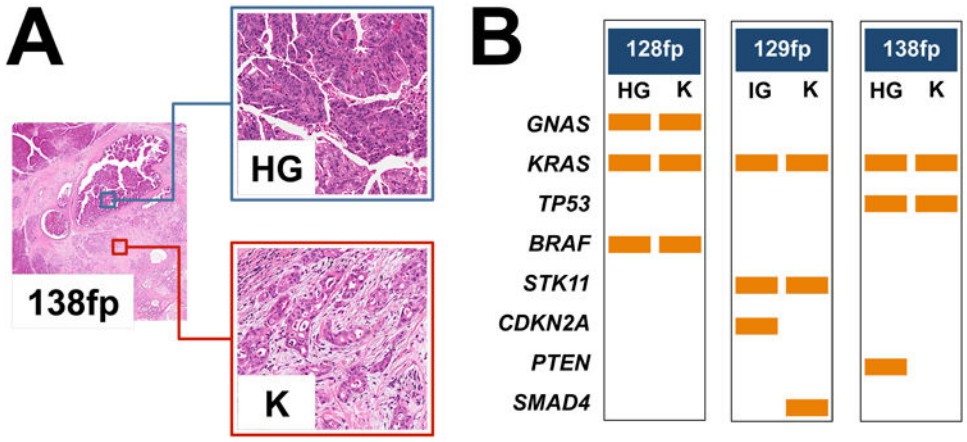

Figure 2. Mutational profiles of matched non-invasive and invasive IPMN components identified by Ion Torrent sequencing

(**A**) Three cases (128fp, 129fp and 138fp) presented a non-invasive intermediate-grade (IG) or high-grade (HG) dysplastic component and an invasive adenocarcinoma (K) component, both of which were analysed using the 50 genes Ampliseq Hotspot Cancer Panel. Representative H&E images from case 138fp are presented (original magnifications 2× and 20×). (**B**) For each pair of samples the first column denotes mutations detected in IG or HG dysplastic samples and the second column represents mutations detected in cancer samples. Rows are the genes in which mutations were detected, and the orange bars represent the mutation. Seven mutations observed in the *GNAS*, *KRAS*, *BRAF*, *KRAS* and *STK11* genes were common to both samples; three mutations were observed in only one of the matched lesions.

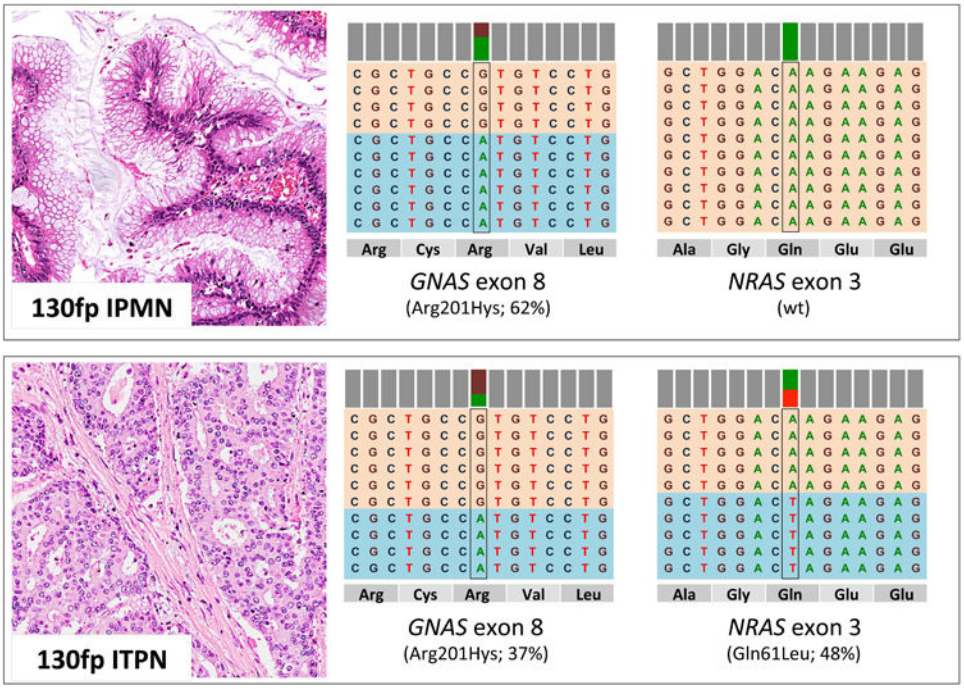

Figure 3. Concomitant IPMN and ITPN sharing a common *GNAS* mutation

Patient 130fp presented two different neoplastic lesions, an intestinal-type IPMN and an ITPN coexisting in pancreatic head. The two phenotypically different lesions showed a common *GNAS* R201H mutation; the ITPN component presented a *NRAS* Q61L mutation. Representative H&E images of the lesions are shown (original magnifications, 20×). On the right of each sample is the representation of the reads aligned to the reference genome as provided by the Integrative Genomics Viewer (IGV v.2.1, Broad Institute) software for the hotspots mutations in the *GNAS* and *NRAS* genes.

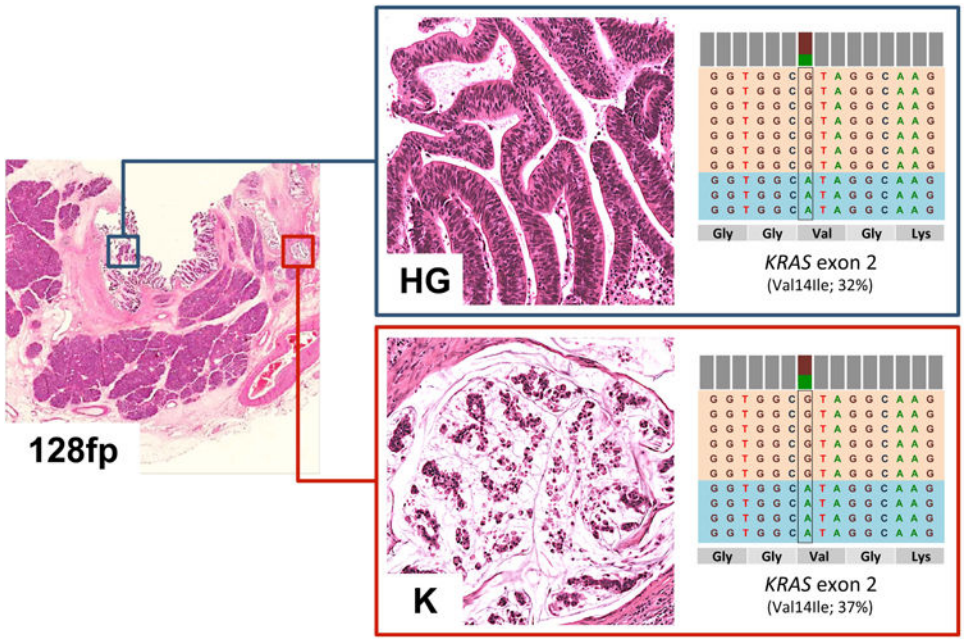

Figure 4. IPMN showing a KRAS mutation V14I

The intestinal-type IPMN 128fp presented a V14I *KRAS* mutation in both the high grade (HG) dysplastic and the invasive carcinomatous (K) component, analysed separately using the 50-gene Ampliseq Hotspot Cancer Panel. Representative H&E image of the lesions is shown (original magnifications, 20×). On the right there is the representation of the reads aligned to the reference genome as provided by the Integrative Genomics Viewer (IGV v. 2.1, Broad Institute) software.

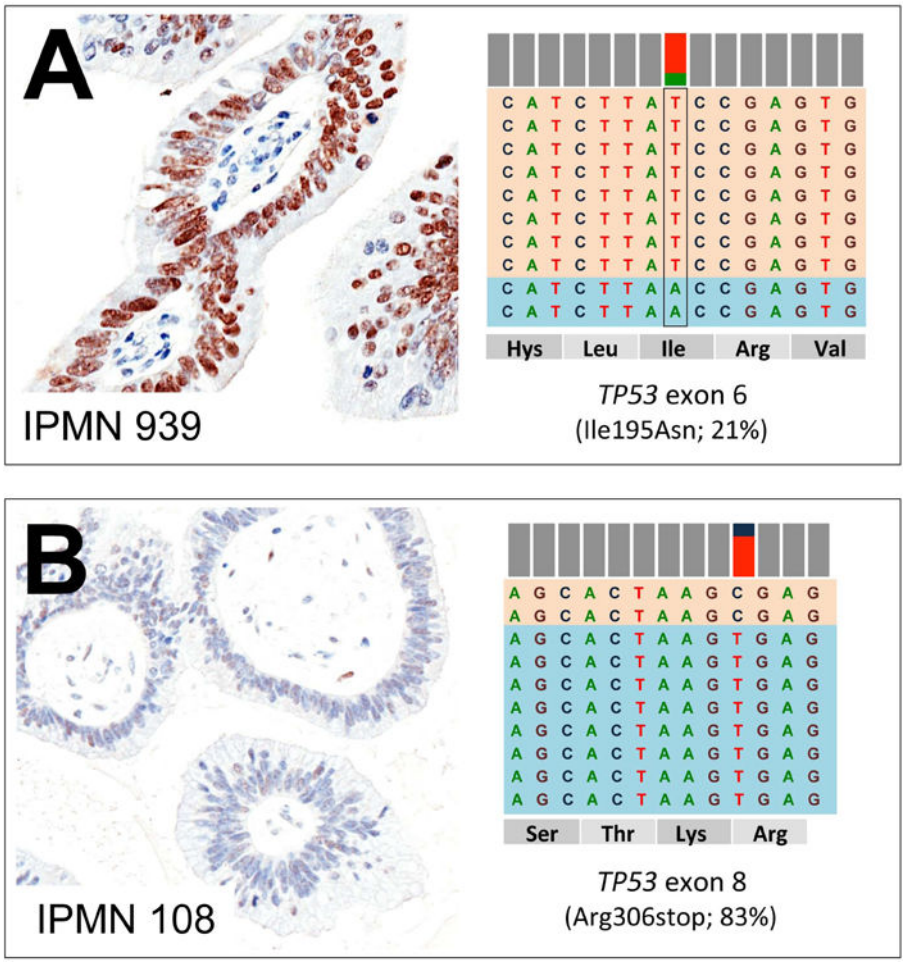

Figure 5. *TP53* mutational status corresponds to p53 protein accumulation

(**A**) Case 939 showed a heterogeneous pattern of staining which is consistent to *TP53* mutational status (21% of mutated alleles, I195N). (**B**) Case 108 with no evident p53 labelling corresponds to a homozygous stop mutation (83% of mutated alleles, R306*). For each sample a representative p53 immunohistochemical image (original magnifications ×20) and the representation of the reads aligned to the reference genome as provided by the Integrative Genomics Viewer (IGV v.2.1, Broad Institute) software are presented.

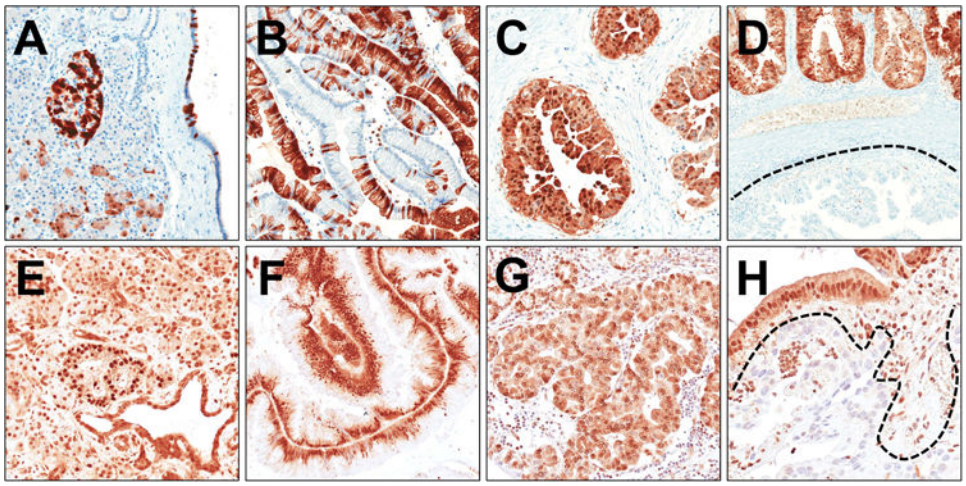

Figure 6. P16 and Smad4 immunoexpression in IPMN

Representative images of p16 (**A-D**) and Smad4 (**E-H**) immunoreactions are shown. (**A**) In normal pancreatic parenchyma, p16 is expressed in Langerhans' islets, and in random acinar and duct cells. (**B**) A barcode-like p16 positivity in a gastric-type IPMN. (**C**) Strong nuclear and cytoplasmic p16 expression in an oncocytic-type IPMN. (**D**) p16 expression heterogeneity in a case of pancreatobiliary-type IPMN (positive and negative p16 components are evident). (**E**) Normal pancreas shows a strong Smad4 expression in all epithelial and stromal cell types with stronger positivity in Langerhans' islets. Strong Smad4 expression in intestinal-type (**F**) and oncocytic-type (**G**) IPMNs. (**H**) A Smad4 negative invasive carcinoma infiltrating the stroma surrounding a pancreatobiliary-type IPMN. Original magnifications 10× and 20×.

Table 1

Demographic and histopathological data of the series of 52 intraductal neoplasms of the pancreas from 51 patients.*

Gender	Male	34 (67.3%)
	Female	17 (32.7%)
Age	Average	64±10 (median 65; range 42-80)
Site	Head	19 (36.5%)
	Uncinate process	2 (3.8%)
	Head/-Uncinate process	19 (36.5%)
	Body-Tail	9 (17.3%)
	Diffuse	3 (5.8%)
Distribution	Main-Duct type	31 (59.6%)
	Branch-Duct type	3 (5.8%)
	Combined	18 (34.6%)
Histotype	IPMN-Gastric	6 (11.5%)
	IPMN-Intestinal	36 (69.2%)
	IPMN-Pancreaticobiliary	3 (5.8%)
	IPMN-Oncocytic	3 (5.8%)
	ITPN	4 (7.7%)
Lesion	Low-Grade	3 (5.8%)
	Intermediate-Grade	17 (32.7%)
	High-Grade	28 (53.8%)
	Adenocarcinoma	4 (7.7%)
Associated carcinoma	Colloid Carcinoma	18 (34.6%)
	Tubular Carcinoma	12 (23.1%)
	None	22 (42.3%)

*One male patient had two coexisting lesions, one IPMN and one ITPN; IPMN, intraductal papillary mucinous neoplasm; ITPN, intraductal tubulopapillary neoplasm.

Table 2

Mutational profile of non-invasive and invasive components in three cases of IPMN with associated carcinoma.

Sample	Subtype	Lesion	*GNAS*	*KRAS*	*TP53*	*BRAF*	*STK11*	*CDKN2A*	*PTEN*
#128fpB	Intestinal	HG dysplasia	R201H (38%)	V14I (37%)		K601E (33%)			
#128fpA	Intestinal	Colloid carcinoma	R201H (27%)	V14I (32%)		K601E (28%)			
#129fpB	Intestinal	IG dysplasia		G12V (42%)			E199D (58%)	V115M (7%) P70L (9%)	
#129fpA	Intestinal	Colloid carcinoma		G12V (16%)			E199D (57%)		
#138fpA	Pancreaticobiliary	HG dysplasia		G12D (44%)	V272L (81%)				Q171* (74%)
#138fpB	Pancreaticobiliary	Tubular carcinoma		G12D (23%)	V272L (31%)				

Note: IG, intermediate grade; HG, high grade. Mutated alleles percentages are shown in parentheses.

Table 3

Mutational profiling of the 52 intraductal pancreatic neoplasms according to pathological data.

Genes	Total (n=52)	Gastric (n=6)	Intestinal (n=36)	Pancreaticobiliary (n=3)	Oncocytic (n=3)	ITPN (n=4)	LG (n=3)	IG (n=17)	HG (n=28)	Carcinoma (n=4)	LG + IG (n=20)	HG + Carcinoma (n=32)
GNAS	38 (73%)	6 (100%)	30 (83%)	1 (33%)	1 (33%)	1 (25%)	3 (100%)	15 (88%)	17 (61%)	4 (100%)	18 (90%)	21 (66%)
KRAS	24 (46%)	5 (83%)	14 (39%)	2 (67%)	2 (67%)	0	2 (67%)	11 (65%)	9 (32%)	2 (50%)	13 (65%)	11 (34%)
TP53	5 (10%)	0	3 (8%)	2 (67%)	0	0	0	0	5 (18%)	0	0	5 (15%)
BRAF	3 (6%)	0	3 (8%)	0	0	0	0	0	2 (7%)	1 (25%)	0	3 (9%)
CTNNB1	2 (4%)	0	2 (6%)	0	0	0	0	1 (6%)	1 (4%)	0	1 (5%)	1 (3%)
IDH1	2 (4%)	0	2 (6%)	0	0	0	0	1 (6%)	1 (4%)	0	1 (5%)	1 (3%)
STK11	2 (4%)	0	2 (6%)	0	0	0	0	1 (6%)	1 (4%)		1 (5%)	1 (3%)
PTEN	2 (4%)	1 (17%)	0	1 (25%)	0	0	0	1 (6%)	1 (4%)	0	1 (5%)	1 (3%)
ATM	1 (2%)	0	1 (3%)	0	0	0	0	0	1 (4%)	0	0	1 (3%)
CDH1	1 (2%)	0	1 (3%)	0	0	0	0	0	0	1 (25%)	0	1 (3%)
CDKN2A	1 (2%)	0	1 (3%)	0	0	0	0	1 (6%)	0	0	1 (5%)	0
FGFR3	1 (2%)	0	1 (3%)	0	0	0	0	0	1 (4%)	0	0	1 (3%)
NRAS	1 (2%)	0	0	0	0	1 (25%)	0	0	1 (4%)	0	0	1 (3%)
SMAD4	1 (2%)	1 (17%)	0	0	0	0	0	1 (6%)	0	0	1 (5%)	0
SRC	1 (2%)	0	1 (3%)	0	0	0	0	0	0	1 (25%)	0	1 (3%)

Note: LG, low-grade dysplasia; IG, intermediate grade dysplasia; HG, high grade dysplasia. ITPN, intraductal tubulo-papillary neoplasm